Experimental Studies on a New Array Design and Maximum Power Tracking Strategy for Enhanced Performance of Soiled Photovoltaic Systems

Dhanup S. Pillai, *Member, IEEE*, J. Prasanth Ram, *Member, IEEE*, Juan Lopez Garcia, Young-Jin Kim, *Senior Member, IEEE,* and João P. S. Catalão, *Fellow, IEEE*

***Abstract*— Soiling poses a significant challenge to the performance of photovoltaic (PV) systems in desert climates. This phenomenon can be attributed to three primary factors: 1) the accumulation of non-dispersed shades, 2) the emergence of multiple power peaks, and 3) the inability of conventional maximum power point trackers (MPPTs) to locate the global MPP (GMPP). To address these issues, this study proposes a new array design that disperses shades caused by soiling through the relocation of PV modules. Distinct to existing works, this method not only enhances power delivery during soiling conditions but also ensures inverter-friendly MPP tracking by aligning the GMPP with the array's open circuit voltage. This alignment is crucial for eliminating voltage fluctuations, allowing even conventional MPPTs to effortlessly track the GMPP without the need for complex tracking algorithms. Furthermore, an advanced tracking strategy has also been proposed to improve the tracking speed. For validation purposes, both shade dispersion and GMPP tracking capabilities of the proposed method are fully tested using various soiling shade profiles. The results clearly demonstrate that this developed methodology offers the flexibility to operate the PV array in both MPP and constant power generation modes, making it highly advantageous for grid-connected applications.**

***Index Terms*— Photovoltaic (PV), maximum power point (MPP), reconfiguration and interconnection schemes**

I. Introduction

GLOBAL energy crisis has fostered the penetration of photovoltaic (PV) systems to conventional power grids, and has been instrumental in meeting the increasing power demands [1]. However, PV system operation is often challenged by meteorological changes and raises major concerns on system reliability [2]. Particularly, in desert climates, partial shade events induced by non-homogenous soiling reduce power generation by almost 4%, even with optimized cleaning scenarios [3]. Therefore, attaining maximum power during such conditions becomes mandatory, which is usually achieved using dedicated maximum power point trackers (MPPTs). However, tracking the global maximum power point (GMPP) is complicated due to the presence of multiple power peaks in the I-V curve [3]. Moreover, as MPPTs cannot enhance the overall power availability from a shaded PV array, new array design strategies that could improve the power performance and guarantee a reliable GMPP tracking seem to be a more viable option for addressing this issue worldwide.

To better understand the importance of GMPP tracking and its barriers during shade scenarios, a literature study is presented. Conventional MPPT algorithms like Perturb and Observe (P&O) [4], Hill Climbing [5], and Incremental Conductance [5], integrated with most commercial inverters operate at the rightmost power peak (RPP) near the open circuit voltage (V_{oc}) in an I-V curve, irrespective of whether it is a local MPP (LMPP) or global MPP (GMPP) [6]. As it is, in most shade cases, GMPP operation is not guaranteed [7]. On the other hand, optimization algorithms like Particle Swarm Optimization (PSO) [7], Flower Pollination Algorithm (FPA) [8], Jaya-differential Evolution (DE) [9], DE-PSO [10], Fireworks algorithm [11], Firefly algorithm[12], Ant colony algorithm [13], Spline control [14] and Hybrid approaches in [15]–[18] are reliable to track GMPP, even during shade events. Unfortunately, these techniques employ extensive I-V curve scanning, usually associated with high voltage and power oscillations, serious computational burden, and complex parameter tuning [4]. Besides, grid-connected PV inverters are generally deployed with P&O for reliable operation with voltage stability [6].

In addition to the above, inverters must also operate in constant power generation (CPG) mode in case of excess power availability. Thus, grid-connected inverters either operate in CPG or MPP mode based on the incident irradiance on the collector plane [19]–[21]. Note that the P&O algorithm is mandatory to realize the CPG mode and is usually termed the CPG-P&O technique in literature [20]. The above observations suggest the benefits of having the GMPP near to V_{oc} (RPP) for inverter friendly GMPP tracking with guaranteed CPG operation, even in partial shade conditions. Though GMPP tracking can be easily achieved by having the GMPP as RPP, it would not be possible to realize the same

This research was supported by Technology Development Program to Solve Climate Changes through the National Research Foundation of Korea (NRF) funded by the Ministry of Science, ICT (2021M1A2A2043894), and the work of J. P. Ram was supported by the National Research Foundation of Korea funded by the Ministry of Science and ICT under Grant 2020H1D3A1A04079991. (*D.S. Pillai* and *J.P. Ram* are co-first authors) (*Corresponding Authors: J.P.Ram & Y.J. Kim*)

J. Prasanth Ram is with the Department of Electrical Engineering, Pohang University of Science and Technology, Pohang 37673, South Korea (e-mails: drjppram@postech.ac.kr).

Dhanup S. Pillai and Juan Lopez Garcia are with the Qatar Environment and Energy Research Institute, Hamad Bin Khalifa University, Qatar Foundation, Doha– Qatar 34110.(e-mails: dsomasekharanpillai@hbku.edu.qa, jlopezgarcia@hbku.edu.qa).

Young-Jin Kim is with the Energy systems Laboratory, Department of electrical Engineering, Pohang University of Science and Technology, Pohang 37673,South Korea, and also with the Institute for Convergence Research and Education in Advance Technology, Yonsei University, Seoul 03722, South Korea (e-mail: powersys@postech.ac.kr).

João P. S. Catalão is with the Research Center for Systems and Technologies (SYSTEC), Advanced Production and Intelligent Systems Associate Laboratory (ARISE), Faculty of Engineering, University of Porto, 4200-465 Porto, Portugal (e-mail: catalao@fe.up.pt).

This article has been accepted for publication in IEEE Transactions on Power Electronics. This is the author's version which has not been fully edited and content may change prior to final publication. Citation information: DOI 10.1109/TPEL.2023.3321601

using conventional series-parallel (SP) module interconnection schemes. Also, SP interconnection significantly reduces the power output during partial shade conditions [22]. Therefore, this research proposes a new total cross tied (TCT) PV array design architecture. The approach is to perform permanent circuit rewiring during the commissioning stage based on a pre-defined mathematical strategy, such that the overall shade profile is effectively dispersed over the entire PV array. To be specific, rewiring is performed by virtue of a new mathematical procedure, named as the "Sum Of Position Squares" (SOPS) technique. Once the architecture is modified, the modules are electrically connected in such a way that the total deliverable power is pointedly improved and the GMPPs are always relocated near to the V_{oc}. In summary, the prime benefits of adopting such a strategy are: 1) power enhancement during shaded/soiled conditions, 2) smoother output I-V characteristics, 3) easy and flexible GMPP tracking, and 4) cost effectiveness. Note that the proposed rewiring method is specifically applicable to the central inverter configuration and the two-stage power conversion process. Additionally, it's essential to emphasize that the dispersion of soiling shade is limited in its applicability to micro-inverters. The re-wiring approach offers the following distinct advantages in mitigating the effects of soiling shade in conventional setups compared to microinverters (i) cost – effectiveness, (ii) greater flexibility in operational modes (iii) Enhanced efficiency, and (iv) enhanced ease of maintenance [22], [23]. More details on rewiring PV arrays with different applications other than the proposed ones can be found in [24]–[26].

Further to the aforesaid improvements, a modification has also been introduced to the P&O algorithm. Since the convergence time of the conventional P&O method is high, a two-stage P&O method is applied in this work. In the first stage, tracking is performed with an adaptive step size and is later switched back to the conventional mode with a reduced step size once the GMPP region is identified. Detailed simulation and hardware tests have been performed in this paper to verify the compatibility of the proposed convention utilizing four different test shade cases.

Based on the investigations carried out, the innovations and novel contributions of this work can be summarized below:

- A new array design architecture has been developed to mitigate the shade effects due to soiling in PV systems.
- The proposed approach not only enhances the power output, but also improves the GMPP tracking efficiency of inverters during multiple shade conditions.

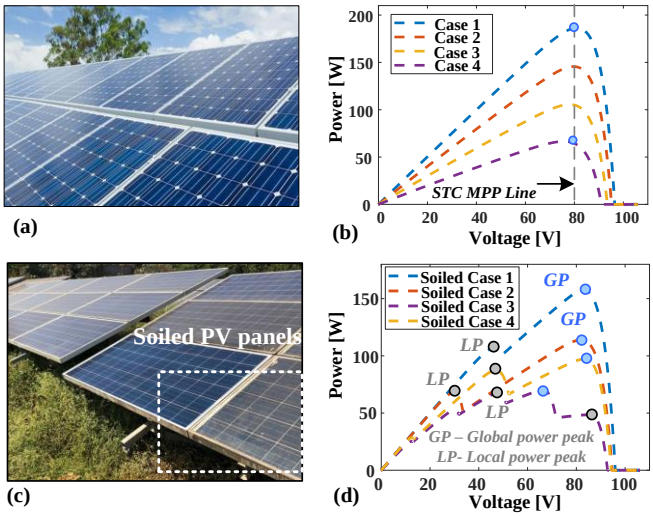

Fig.1. Normal operating conditions (a) PV array, (b) P-V characteristics, Soiled conditions - (c) PV array and (d) P-V characteristics.

- The SOPS algorithm-based rewiring produces smooth power-voltage characteristics (resembling a single peak curve) and relocates GMPP to a voltage near to the V_{oc}.
- An improved and adaptive P&O method that tracks GMPP with better convergence time has been conceptualized.
- The proposed concept has a key application towards CPG operation in grid-connected PV arrays that always guarantees GMPP operation in CPG mode.

II. Importance of Inverter Friendly MPP Operation in Soiled PV Arrays

Soiling is a challenging phenomenon, especially for those PV systems located in desert climates [3]. To understand the effect of soiling, a simple PV array (illustrative only) under normal/uniform operating conditions is presented in Fig.1 (a) and its expected P-V curves at various irradiance levels are presented in Fig.1 (b) respectively. As can be seen, an unsoiled PV array possesses simple operating regions with a unique MPP point to facilitate easy power conversion. It is important to mention that Fig. 1 only intends to create an understanding of a practical scenario for the readers, and the I-V characteristics are not representative of the exact pattern seen. Similarly, the soiled PV array shown in Fig.1 (c) is expected to produce much-complicated P-V characteristics based on various shading patterns that can be created due to the accumulation of dust. For which, some examples are shown in Fig.1 (d). Thus, it is obvious that the P-V characteristics of a soiled PV array are identical to those with

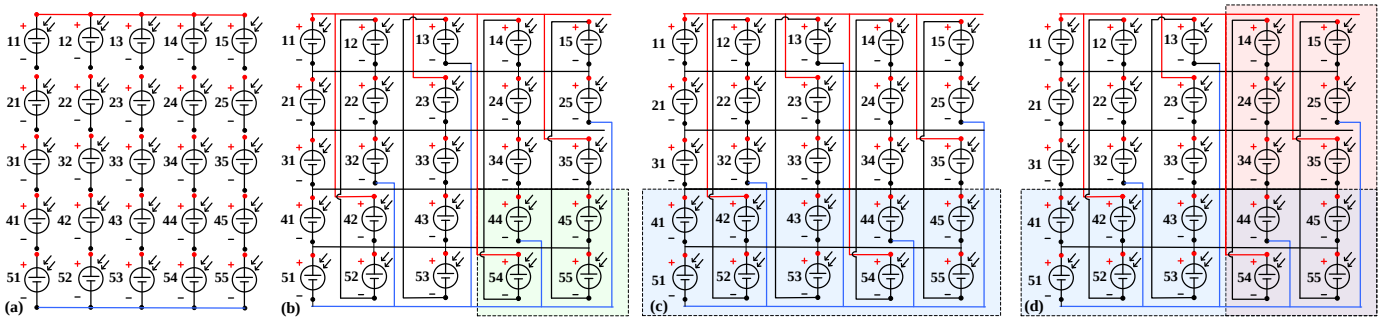

Fig.2. 5×5 PV arrangement for (a) conventional series – parallel connection, rewired TCT in soiled conditions: (b) low (4 modules shaded), (c) moderate (10 modules shaded), and (d) heavy shading (16 modules shaded)., Note: wiring color– +Ve rail– red, -Ve rail-blue.

This article has been accepted for publication in IEEE Transactions on Power Electronics. This is the author's version which has not been fully edited and content may change prior to final publication. Citation information: DOI 10.1109/TPEL.2023.3321601

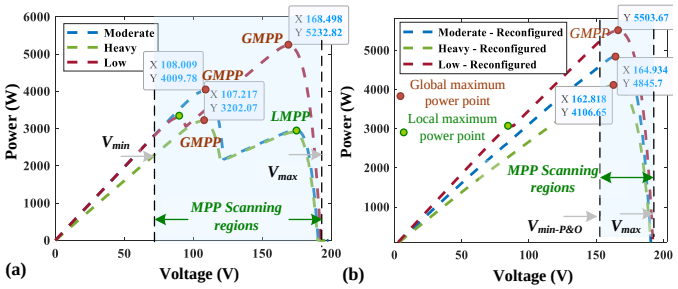

Fig .3. PV characteristics of (a) Conventional, and (b) reconfigured PV array.

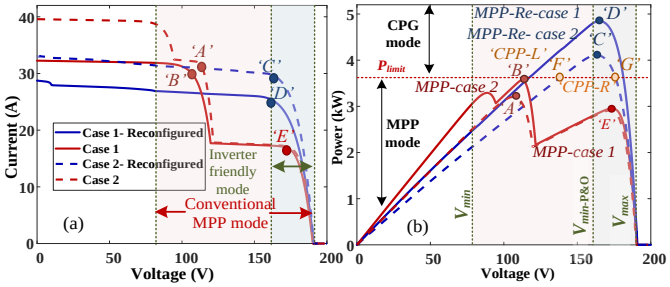

Fig.4. Illustration of CPG and MPP modes in conventional SP and rewired TCT interconnected PV array: (a) I-V and (b) P-V characteristics.

partial shade conditions, and hence, can be modeled identically. However, it is important to mention that no data is available in the literature pertinent to the non-homogenous soiling patterns recorded onsite. As it is, one future scope of this work would be to identify real-world soiling patterns and test the proposed approach for the same patterns. Therefore, the soiling patterns used in this work are those widely assumed in the literature itself [28].

In contrast to shading, soiling demands different mitigation methods – usually manual or robotic cleaning of PV modules [29]. However, the power conversion efficiency even after deploying cleaning mechanisms depends on the frequency of the cleaning cycles. In this context, note that this work is not an alternative mitigation approach for soiling. Rather, the objective is to enhance the power performance during soiled conditions in non-cleaned systems and also between cleaning cycles in cleaning-deployed systems, which subsequently helps to optimize the cleaning schedules based on the power generated. Thus, in a nutshell, the idea is to reduce the shade effect due to soiling to enhance power generation. However, as mentioned earlier, MPP tracking also plays a crucial role in achieving this task.

To understand the MPP tracking and its complexity during soiled cases, discussions on the reconfigured PV arrangement along with conventional PV arrangement are elaborated further. Note that, in conventional PV arrangements, most PV inverters equipped with conventional tracking algorithms fail to track GMPP during soiling/shading conditions. To better understand this effect, three various soiling events namely low, heavy, and moderate shading have been modeled in a 5×5 TCT interconnected PV array (with 100 W PV modules). The definition of heavy, moderate, and low soiling cases is derived based on the number of irradiance changes, and the total number of modules involved in irradiation change. As the number of irradiance changes increases, the complexity of the P-V curve also increases since the number of bypasses and thereby, the number of power peaks in the output characteristics increase. Note that the shading levels based on the irradiance changes are the only criterion used for comparison between different cases.

For a better understanding of rewiring, the conventional PV arrangement, and the reconfigured PV array in three different shade events are presented in Fig. 2(a)–(d), respectively. For identification, the positive rail of a PV panel in a string is marked by 'red' wire, and the negative rail with blue color. Furthermore, to explain the PV array reconfiguration and its impact on PV characteristics, the numerical procedure adopted in [1] is considered here to better understand the shade dispersion. Similar shade profiles are also verified for the proposed rewiring scheme in the following sections, to test the shade dispersion ability with the proposed rewiring scheme. For the given shade patterns, the corresponding P-V characteristics obtained for each case are presented in Fig. 3(a) and (b) respectively. As seen from the P-V characteristics, except for case 3 (low shading), the GMPP is not the RPP. As a result, the tracking efficiency decreases and additional power is lost, thereby aggravating the issue of soiling. Furthermore, for cases 1 and 2 (moderate and heavy shading), GMPPs are observed at a voltage nearly equal to 0.4 V_{oc}, mandating a broader voltage band search for attaining GMPP, even if advanced algorithms are deployed.

On the other hand, when the array design is modified by changing the electrical interconnections within a TCT approach as in Fig.2 (c)-(d), the overall power performance in each case has been significantly improved (see Fig.3 (b)). More importantly, the GMPPs are now relocated as RPPs with a much linear PV characteristic resembling uniform shade cases. The relocation is so significant that the inverters always operate at the GMPP, and the power enhancement is achieved with a limited voltage band search itself, which is particularly helpful in grid-connected systems.

The voltage band search limits in conventional and rewired PV array are expressed in (1). With the above benchmark findings, a reliable array design compatible with all shade profiles is conceptualized in section III.

$$V_{PV} = \begin{cases} V_{min} - V_{max}, \ for \ SP \ PV \ array \\ V_{min-P\&O} - V_{max}, for \ reconfigured \ PV \ array \end{cases} \quad (1)$$

A. Achieving CPG and MPP modes:

In grid-connected systems, both CPG and MPP operation modes are essential based on the constraints given in Eqn. 2 [19]. The system is supposed to operate in the CPG mode (P_{CGP}) when PV power generation (P_{PV}) exceeds the grid limits (P_{limit}) and in MPP mode (P_{MPP}) otherwise. For a detailed understanding on CPG and MPP modes, readers may refer to [2], [20].

$$P_{PV} = \begin{cases} P_{MPP}, when \ P_{PV} \leq P_{limit} \\ P_{CGP}, \ when \ P_{PV} \geq P_{limit} \end{cases} \quad (2)$$

To understand the relevance of array design modification to grid-connected systems, two random shade events (case 1 and 2 in Fig.2) are considered. For the same test cases, the I-V and P-V characteristics obtained for conventional SP, and rewired TCT design are shown in Fig.4 (a) and (b) respectively. Furthermore, the MPP and CPG modes are highlighted as well as the voltage band requirement to operate at GMPP.

From which, the following observations are evident: 1) power generation from conventional interconnected PV array

This article has been accepted for publication in IEEE Transactions on Power Electronics. This is the author's version which has not been fully edited and content may change prior to final publication. Citation information: DOI 10.1109/TPEL.2023.3321601

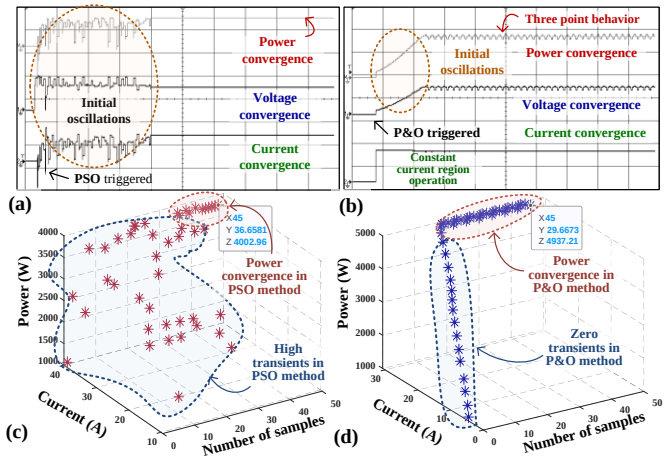

Fig.5. Experimental results for MPP tracking - (a) PSO method, (b) P&O method; Switching transient 3D plot - (c) PSO method (d) P&O methods.

is significantly low for both cases (below P_{limit}), and hence CPG operation mode is not possible, 2) locating GMPPs for SP interconnection during dynamic shade occurrences (marked as 'A' and 'B' respectively for cases 1 and 2) is difficult, and a broader search region within the I-V curve becomes mandatory (indicated as V_{max} and V_{min}) for MPP operation, 3) the rewired TCT configuration enhances the power generation substantially for both cases, 4) array modification mitigates the issue of multiple peak occurrences, and 5) rewiring relocates GMPPs as RPPs (points 'C' and 'D'), and eases the GMPP search process and the region (V_{max} and $V_{min-P\&O}$). In summary, by relocating GMPPs, both CPG and MPP modes can be achieved using the conventional P&O tracking algorithm itself with better power generation.

B. Significance of P&O in inverter-friendly tracking:

If the P&O method is implemented for the shade events (Case 1 &2) with a duty cycle value of 0.1 (constant voltage regions) in the case of a conventional PV array, it is likely to get settled to the right most local power peaks (marked as 'E' for cases 1 and 2 in Fig.4), whereas the same on a rewired PV array is expected to track the relocated GMPP points (RPPs 'C' and 'D'). To verify this, the P&O tracking pattern is experimentally verified for case 1 on a laboratory prototype (details provided in section VI). Furthermore, to evaluate the impact of switching transients, the performance is compared with a particle swarm optimization (PSO) algorithm. Note that PSO is applied to the SP interconnected system to illustrate the power difference.

From the results shown in Fig. 5, it is evident that rewiring has had notable power enhancement, and P&O easily locates and settles to the GMPP (RPP). Another notable improvement is that P&O method has very fewer switching transients, while the PSO method shows significant transients and oscillations prior to reaching convergence. For clarity on the significance of switching transients, the first 50 samples of PSO and P&O methods for shade case 1 are considered as a function of power and voltage and plotted as three-dimensional charts in Fig.5 (c) and (d) respectively. It is seen that the PSO method has wide unsettled power and voltage oscillations for a long

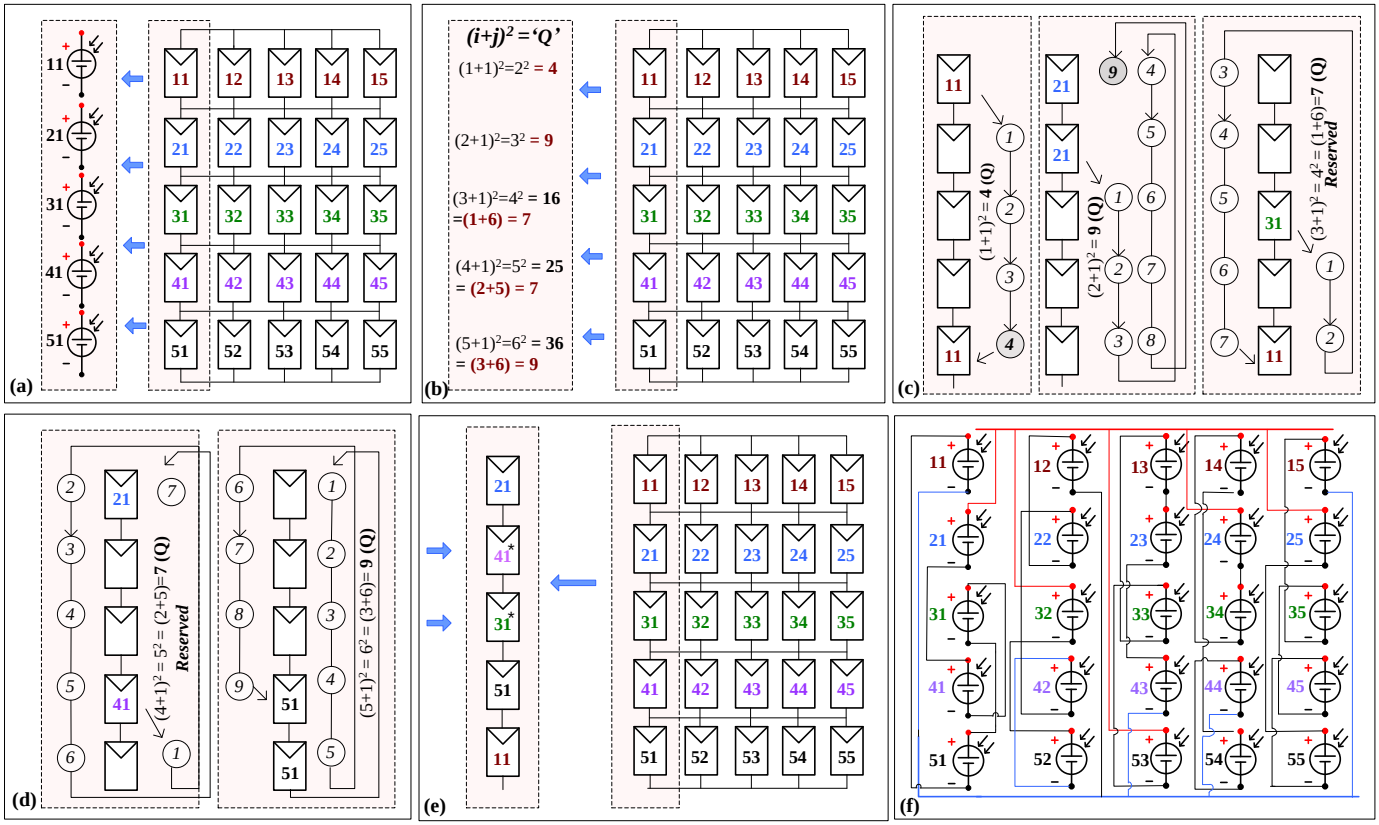

Fig.6. Illustration of the SOPS method–5 × 5 PV array: (a) simple TCT interconnection, (b) determining 'Q' value for the first column based on SOPS procedure, (c) re-wiring the first column elements '11', '21' and '31', (d) re-wiring the first column elements '41' and '51', (e) illustration of the '*reserved*' PV panels in the first column, and (f) the final PV arrangement of SOPS-PV arrangement. (Note: wiring color– +Ve rail– red, -Ve rail -blue)

time, while a flat and steady convergence is observed with the P&O method.

Note that the flexibility to operate in CPG mode (at P_{limit}) is also a noticeable advantage of relocating the GMPP in grid-connected systems. However, experimental discussions on CPG mode are not performed since it is out of the scope of this work.

III. Proposed Array Design and Tracking Approach

The previous discussions exemplify dynamic performance degradation in PV arrays during soiled/shaded conditions and the impact of power enhancement and inverter-friendly MPP tracking that could be achieved via rewiring a TCT based PV array. However, not all reconfiguration approaches provide similar benefits, and such an algorithm would be competent enough to enhance power generation by dispersing the shades in such a way that the RPP is always GMPP, irrespective of the incident shade pattern. Another key compatibility indicator in TCT interconnected rewiring is row current difference minimization [1]. To achieve the above objectives, a new SOPS algorithm-based array design is proposed in this article. Furthermore, an enhanced P&O tracking approach is also developed. For modeling and validation, a 5×5 PV test system is considered since the proposal seems to be ideal for small-scale systems in a microgrid environment.

A. SOPS Approach for Rewiring

The proposed SOPS method is a simple mathematical approach to rewire the PV modules based on their initial position indices. For brevity, let us consider the position of a module expressed as 'ij', where 'i' refers to the row and 'j' to the column numbers (see the positions indicated in Fig.6(a)). Note that to avoid wiring complexities, only column-wise rewiring is intended to be performed. The procedure starts by obtaining the SOPS value of each module to be relocated, by determining the numerical value of $(i+j)^2$.If the resultant value is a single digit number (Q), the respective module is assumed to be relocated to an 'Q' number of places vertically downwards (see Fig. 6(b)). If $(i+j)^2$ yields a double-digit number (say with digits 'mn'), the number of vertical displacements required is determined by performing sequential additions, (say $m+n=Q$) until a single digit is obtained. Once the new positions are identified, the electrical connections are altered to maintain the same 'Q' number of module locations within the column.

The rewiring process within the first column elements of the considered 5×5 PV array based on the SOPS values is graphically shown in Fig.6(b). From this, it is observed that the module with position '11' is electrically relocated to position '51'. Similarly, module '21' is relocated nine places sequentially to position '11'. On the other hand, for module '31', the SOPS value is '16', and henceforth, the relocation needs to be performed by 7 places (refer to Fig.6(c)). As can be seen, if the preferred position is preoccupied (in this case '11'), the respective step is reserved for a later relocation after completing all possible steps. A similar case is seen for module '41' as well as illustrated in Fig.6 (d). As it is, module '51' is first relocated (Fig.6(d)), and then, the previously reserved modules ('41' and '31') are allocated to the empty places in descending order as shown in Fig.6.(e). Identically, the remaining columns are also rewired, and the resultant interconnection is shown in Fig.6 (f).

B. SOPS Rewiring – Step-wise procedure

Assuming the variable 'i' as the row number and the variable 'j' as the column number of the PV module, 'ij' denotes the PV module position in the PV array. For instance, number '52' denotes the PV panel located in the 5_{th} row and 2_{nd} column.

Step 1: *Sum of Position Square (SOPS):* For the given PV array, perform SOPS $(i+j)^2$ for each PV panel to determine the single-digit numerical value 'Q'. If the result of $(i+j)^2$is a double-digit number, denoted as 'mn', perform sequential additions of the digits $(m+n)$ until a single digit 'Q' is obtained, which determines the number of vertical displacements required (see Fig. 6(b));

Step 2: *Vertical displacements (re-wiring) in strings*: For the

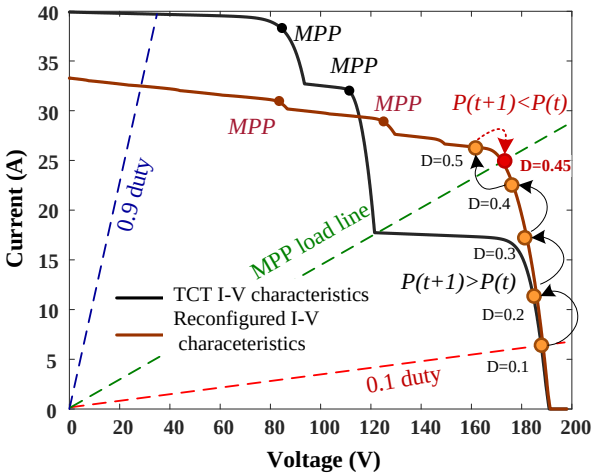

Fig.7. I-V characteristics of TCT and rewired PV array.

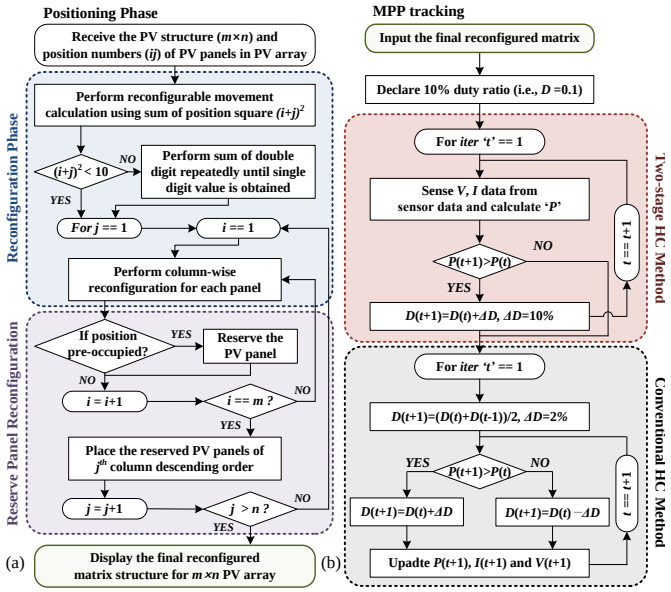

Fig.8. Generalized flowchart for (a) SOPS Approach and (b) two-phase / adaptive P&O tracking.

given PV array, starting from string 1, each PV panel in the string will undergo 'Q' number of vertical displacements to relocate to a new position (see Fig. 6(c));

Step 3: *'reserve' status in relocation:* During relocation, if any of the cells is pre-occupied, 'reserve' the respective PV panel for later relocation. Nevertheless, continue relocating other PV panels in the string via vertical displacements (see Fig. 6(d));

Step 4: *Optimizing the placements for 'reserved' PV panels:* After relocating all the PV panels in a column, the reserved PV panels should be placed in the empty cells in reverse chronological order (see Fig. 4(e)).

Steps 2-4 are repeated for all the strings of the given PV array to achieve the final one-time reconfiguration. It is important to note that the procedure is straightforward and can be applied to any PV array structure to disperse the effect of soiling.

C. Proposed two-step/adaptive GMPP tracking.

Since the proposed SOPS approach guarantees to relocate GMPP to RPP via rewiring, advanced optimization algorithms are no longer required to track GMPP. While the conventional P&O method is sufficient to serve this purpose, it is also important to address the slow convergence associated with P&O-based techniques [27]. Therefore, a few alterations are introduced to the fundamental P&O method to enable fast tracking. The P&O method being a perturbation approach, the change in duty cycle (ΔD) per iteration is a key factor that decides convergence speed. As it is, an adaptive P&O methodology having two various adaptive step sizes in duty cycle perturbation is proposed in this work.

To explain the adaptive approach, the resultant I-V characteristics of the basic TCT and rewired PV array are considered, and the same is shown in Fig.7. From the figure, it is seen that the output characteristics of the rewired PV array become smooth with GMPP relocated as the RPP. Therefore, tracking starts from the right-hand side of the I-V curve, achieved with a duty cycle of 0.1 initialized in the constant voltage region.

Once initialized, the value of ΔD is updated with a higher step size (10%) until reaching the GMPP vicinity (see Fig.7). It can be noticed that the duty cycle is constantly updated from 0.1 to 0.5, and the GMPP region is identified during the update from 0.4 to 0.5. since the operating power of P&O at duty 0.5 is relatively less than that at 0.4. The above steps are mathematically given as:

$$if\ P(t+1) > P(t), D(t+1) = D(t) + \Delta D;\ \Delta D = 10\% \quad (3)$$

where 'P' is the instantaneous power, 't' is the iteration number, and 'D' is the duty cycle. Once $P(t+1) < P(t)$, the value of D is re-declared as the average of $D(t-1)$ and $D(t)$, and also, ΔD is changed to 2%.

$$if P(t+1) < P(t), D(t+1) = \frac{D(t)+D(t-1)}{2};\ \Delta D = 2\% \quad (4)$$

Post re-declaration, the tracker explores the MPP region in a narrow range to locate the GMPP. For a clear understanding of the overall rewiring process assisted by adaptive GMPP tracking, a generalized flowchart is presented in Fig.8.

IV. Numerical Studies

This section presents the implementation of 4 test cases for validating the proposed SOPS rewiring scheme in a 5×5 PV array. The conventional TCT interconnection and SOPS final arrangement for the test system is analyzed for four various soiling profiles, and the trial runs via MATLAB simulation is made to identify the maximum power generation. These four different shade profiles that are likely to emulate real-time dust accumulation events have been considered for evaluations based on the existing literature [24-26, 29]: (i) Short wide (SW), (ii) Long wide (LW), (iii) Long Narrow (LN), and (iv) Short Narrow (SN). Simulations are performed to evaluate the

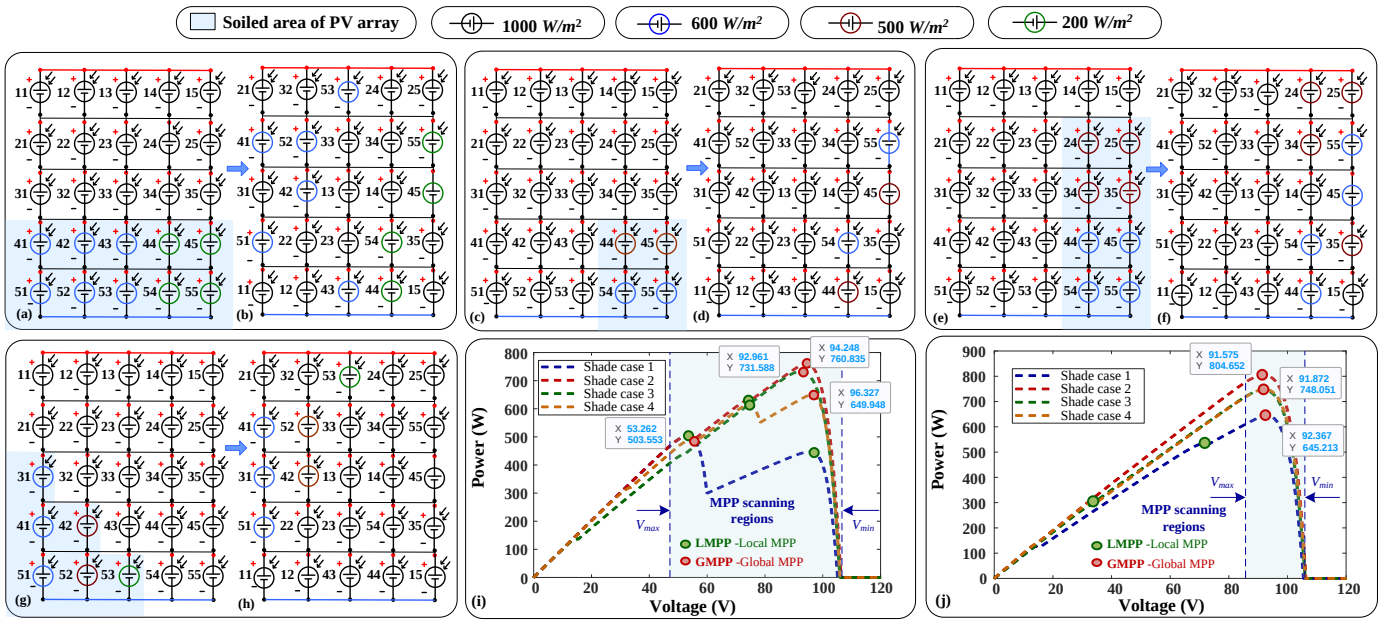

Fig.9. Soiled Case 1: (a) conventional and (b) SOPS PV array; soiled Case 2: (c) conventional and (d) SOPS PV array; soiled Case 3: (e) conventional and (f) SOPS PV array; soiled Case 4: (g) conventional and (h) SOPS PV array; P-V characteristics for Cases 1-4: (i) conventional and (j) SOPS rewired PV array, (Note: wiring color– +Ve rail– red, -Ve rail-blue).

This article has been accepted for publication in IEEE Transactions on Power Electronics. This is the author's version which has not been fully edited and content may change prior to final publication. Citation information: DOI 10.1109/TPEL.2023.3321601

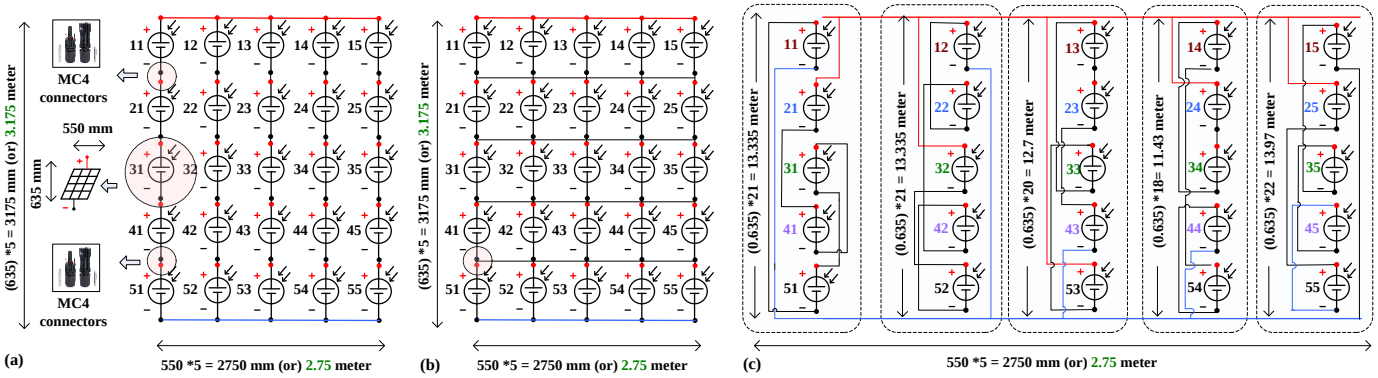

Fig.10. Wiring length and connector requirements for (a) series parallel (SP), (b) TCT and (c) SOPS interconnection, (Note: wiring color– +Ve – red, -Ve-blue).

power performance of SP/TCT and the proposed SOPS schemes. For modeling, Shell S36 W modules have been used.

For a detailed understanding of the PV array in different soiling conditions, the representation of conventional and SOPS-rewired PV arrays for four various soiling profiles is presented in Fig.9(a)-(h). Subsequently, the results obtained for conventional, and SOPS technique-based PV arrangement are plotted in Fig .9(i) and Fig.9(j) respectively. Furthermore, the GMPP power values obtained in each case are recorded and indicated in Table I. Pertinent to each shade profile, multiple current changes are created in the conventional system, which subsequently leads to multiple power peaks (see Fig.9 (i)) in the P-V curve. Note that the impact of shade is considerably lower on shade patterns 2 and 3, and simulated P-V characteristics are therefore smoother compared to cases 1 and 4.

On the other hand, owing to the SOPS approach, better output characteristics have been obtained for all shade profiles when the array is rewired, compared with the conventional schemes. More importantly, irrespective of the shade profile, the GMPPs have been relocated to a new RPP in the P-V curve (see Fig. 9(j)). Also, the GMPP power values show substantial improvements. From the tabulated values in Table II, it is worth pointing out that the proposed array design has generated significantly higher power in all the test cases: 142 W, 44 W, 17 W, and 39 W respectively for SW, LW, LN and SN shade profiles.

TABLE I.
GLOBAL MPP VALUES OBTAINED BY CONV. AND SOPS INTERCONNECTION

Soiling case	Configuration	V (V)	I (A)	P (W)
Case 1	Conventional	53.26	9.45	503.55
	SOPS	92.36	6.99	645.21
Case 2	Conventional	92.24	8.24	760.24
	SOPS	91.55	8.79	804.65
Case 3	Conventional	92.93	7.87	731.58
	SOPS	91.87	8.14	748.05
Case 4	Conventional	96.32	6.75	649.94
	SOPS	91.87	8.14	748.05

Conventional – SP / TCT, SOP-sum of position square,

TABLE II
THEORETICAL ROW CURRENT CALCULATION FOR SHADE PATTERNS 1 – 4

Soiling Case	Conventional				Proposed method			
	Row No	I_m (A)	V_m (V)	V_mI_m (W)	Row No	I_m (A)	V_m (V)	V_mI_m (W)
SW Case 1	*R4*	*2.2*	*5*	*11*	*R2*	*3.2*	*5*	*16*
	R5	-	-	-	*R3*	*3.5*	*4*	*14*
	R1	*4.5*	*3*	*13.5*	*R4*	-	-	-
	R2	-	-	-	*R5*	-		-
	R3	-	-	*4.5*	*R1*	*4.3*	*1*	*4.3*
LW Case 2	*R4*	*3.7*	*5*	*18.5*	*R3*	*4.1*	*5*	*20.5*
	R5	-	-	-	*R5*	-	-	-
	R1	*4.5*	*3*	*13.5*	*R2*	*4.2*	*3*	*12.6*
	R2	-	-	-	*R4*	-	-	-
	R3	-	-	-	*R1*	*4.5*	*1*	*4.5*
LN Case 3	*R1*	*1.5*	*5*	*7.5*	*R2*	*3.8*	*5*	*19*
	R4	*3.7*	*4*	*14.8*	*R4*	-	-	-
	R5	-	-	-	*R1*	*3.9*	*3*	*11.7*
	R2	*3.9*	*2*	*7.8*	*R3*	*4.1*	*2*	*8.2*
	R3	-	-	-	*R5*	-	-	-
SN Case 4	*R5*	*3.1*	*5*	*15.5*	*R1*	*3.8*	*5*	*19*
	R4	*3.8*	*4*	*15.2*	*R2*	-	-	-
	R3	*4.2*	*3*	*12.6*	*R3*	-	-	-
	R1	*4.5*	*2*	*9*	*R4*	*4.2*	*2*	*8.4*
	R2	-	-	-	*R5*	*4.5*	*1*	*4.5*

V_m=module voltage, I_m-module current, V_mI_m-array power, SW -Short Wide, LW-Long Wide, LN-Long Narrow, SN-Short Narrow

A. Comparison with conventional TCT and SOPS approaches

TCT interconnection performs identically to the SP scheme unless suitable design approaches are applied. Therefore, to verify the compatibility of the proposed SOPS rewiring design, a theoretical study highlighting the maximum attainable voltage, row current, and power values are performed, and the results are tabulated in Table II. Note that row current difference is a critical parameter controlling the number of bypasses and thereby, the shape and peaks of the I-V characteristic [28].

Therefore, it can be established as a reliable variable to gauge the success rate of the proposed technique. In this context, row currents of TCT and SOPS approach are separately analyzed for each shade profile considered. Note that 'V_m' and 'I_m' values in Table II denote the maximum voltage and current values delivered by each row (marked as R_1 to R_5). From the results, it is evident that the SOPS application has reduced the row current difference considerably, which has helped to improve the curves previously examined in Fig. 9. Also, the GMPP occurrence in the conventional TCT method is not consistent, while the proposed method has always guaranteed to relocate the GMPP to the maximum voltage at RPP ($5\,V_m$). Consequently, independent of the shade patterns, the power coefficient of the SOPS method is always high, which portrays the capability of the developed approach to improve shade dispersion, compared to the conventional array designs. To summarize, the proposed method showcases tremendous potential to

TABLE III
ESTIMATION OF WIRING LENGTH AND CONNECTORS FOR CONVENTIONAL AND SOPS METHODS

Configuration/ Parameters	Conventional		Proposed
	SP	TCT	SOPS
Column wiring length (meter)			
String 1 (or) Column 1	3.18	3.18	13.34
String 2 (or) Column 2	3.18	3.18	13.34
String 3 (or) Column 3	3.18	3.18	12.7
String 4 (or) Column 4	3.18	3.18	11.43
String 5 (or) Column 5	3.18	3.18	13.97
Terminal wiring length (meter)			
+ve terminal	2.75	2.75	2.75
-ve terminal	2.75	2.75	2.75
Cross links wiring length (meter)			
Link 1	-	2.75	2.75
Link 2	-	2.75	2.75
Link 3	-	2.75	2.75
Link 4	-	2.75	2.75
Miscellaneous	2	2	2
Total wiring length	**23.38**	**34.38**	**83.27**
Total MC4 Connectors	50	82	82

TABLE IV
COST COMPUTATION FOR CONVENTIONAL AND SOPS METHODS

Parameters	Conventional (SP)		SOPS	
	Count	**Cost**	Count	**Cost**
WL (meters)	23.38	**24**	**83.27**	**84**
MC4 Connectors	50	**50**	82	**82**
Total cost	**74 (approx.)**		**166 (approx.)**	

WL-wiring length, 10 meter = 10 USD, MC4 cost (1each= 1 USD)

TABLE V
PROGRAMMED SOILED SHADE PATTERN FOR ENERGY SAVING ANALYSIS

Day/ Time	8 AM – 10 AM	10AM – 12 PM	12 PM- 2 PM	2 PM – 4 PM	4PM - 6PM
Day 1	Case 1	Case 2	Case 3	Case 4	Case 2
Day 2	Case 2	Case 3	Case 4	Case 2	Case 2
Day 3	Case 3	Case 2	Case 4	Case 3	Case 1
Day 4	Case 1	Case 4	Case 4	Case 3	Case 3
Day 5	Case 3	Case 4	Case 3	Case 2	Case 2

TABLE VI
ENERGY SAVING AND UNIT GENERATION CALCULATION

Day	PG (kW/hr)		UG		RG (USD)	
	Conv.	SOPS	Conv.	SOPS	Conv.	SOPS
Day 1	6461.02	7182.3	6.46	7.18	77.53	86.19
Day 2	7103.88	7706.9	7.10	7.71	85.25	92.48
Day 3	6825.96	7480.5	6.83	7.48	81.91	89.77
Day 4	7267.16	7706.9	7.27	7.71	87.21	92.48
Day 5	7089.03	7614.4	7.09	7.61	85.07	91.37
Units and revenue generated	**34.75**	**37.69**	**416.9**	**452.29**		

PG- Power generated, **UG**-Units Generated, **RG**-Revenue Generated

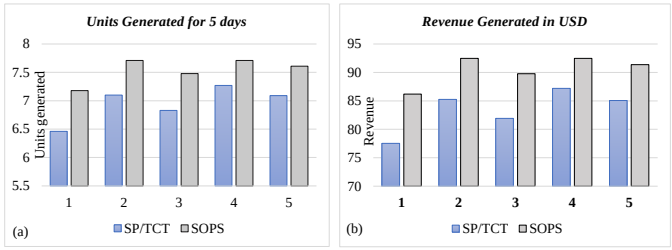

Fig.11. Comparison chart: (a) units, and (b) power generation.

encounter performance degradation issues in soiled/shaded PV arrays.

B. Cost computation analysis

The arrangement of the SOPS configuration, although computationally proven to yield high power in soiled conditions, necessitates a comprehensive explanation for readers due to its lengthy interconnecting ties, sensor requirements, additional terminal connectors, and wiring needs. Therefore, the capital expenditure (CAPEX) cost of the proposed SOPS method for a simple 5×5 PV arrangement has been compared with those of the series-parallel (SP) and Total-Cross-Ties (TCT) interconnections. Since the S36 PV panel is utilized in our research [30], we have derived the dimensions of the PV module from the datasheet to determine the cabling requirements.

Based on the module dimensions, the estimated PV string length for the given 5 modules in portrait orientation of SP and TCT interconnections is depicted in Fig. 10(a) and 10(b) respectively. Note that the CAPEX cost computation also includes real-time MC4 connectors for all the PV modules and the respective interconnection schemes. For SP and TCT interconnections, the estimated cabling length for a string is 3.175 meters, and the row cabling length is 2.75 meters. In the case of TCT interconnection, additional cabling length is considered due to the excess cabling requirement in the cross-link (interconnection ties).

In contrast to conventional PV arrangements, the SOPS configuration demands additional cabling requirements, which vary for each individual string. The estimation of cable length for all the 5 strings in the SOPS approach is presented in Fig. 10(c). Unlike electrical array reconfiguration schemes, the SOPS arrangement is a one-time rewiring scheme; hence, the additional cost for sensors and electronic switches is completely neglected. Despite the additional cable requirements in the strings, the row-wise cabling length remains identical to SP and TCT interconnections. Table III presents the total cabling length and the MC4 connector requirement for SP, TCT, and SOPS PV arrangements. Furthermore, the proposed approach relies only on column-wise relocations, i.e., modules in one column remain in the same column even after relocation. This significantly reduces the overall cost compared to alternative approaches in the literature.

Referring to the wiring and connector requirements in Table III, the cost computation for SP and SOPS arrangements is performed and presented in Table IV. According to various online shopping websites, the cost of PV cable is found to be 10 USD for 10 meters, and each MC4 connector costs 1 USD. According to these cost values, the CAPEX cost for wiring and cabling of SP and SOPS arrangements is determined as 74 USD and 166 USD, respectively. Note that the TCT cost computation is ignored since the SOPS arrangement involves rewiring performed within the TCT itself. On computations, the SOPS arrangement necessitates an additional 92 USD as CAPEX cost, compared to conventional PV systems. Also note that the real benefit of reconfiguration comes from the enhancement in the average energy yield, which has a much higher impact on the Levelized Cost of Energy (LCOE). In fact, the CAPEX of real-world PV systems is already very high, and therefore, additional cost requirements for cabling do not contribute to a significant percentage increase in CAPEX. Instead, considering LCOE as the key figure of merit to assess the system's cost competitiveness, the benefit of

higher yield is more impactful. Discussions on energy savings, income generation, and payback returns that contribute to LCOE are discussed in the next subsection.

C. Energy saving, payback returns and income generation.

To evaluate the power conversion potential of the proposed SOPS array design, an extended power generation analysis is presented as a function of energy saving and income generation. For this analysis, various shade patterns at soiled conditions, which are simulated earlier in this section, are considered. Moreover, the soiled patterns are found randomly repeated in a sequence from morning 8 a.m. – 6 p.m. for a period of 5 days (day 1 – day 5) as shown in Table V. Furthermore, the analysis is performed on the assumption that the PV array is always ensured to operate at MPP for all the shade patterns. The analysis intends to provide an overview of the payback returns for the additional cost (92 USD) consumed in CAPEX investment of SOPS arrangement.

Given the MPP values plotted in Fig. 9., various data like total power generation (kW/hr), units generated, and revenue generation are calculated as shown in Table VI. Note that the units are only estimated after carefully evaluating the effective sun hours (i.e., 8) daily. From the tabulated data, the conventional system has generated 34.75 units and the SOPS array has generated 37.69 units respectively. On calculating the total revenue generated at 12 USD per unit, the conventional and SOPS PV arrangements have earned 416.9 USD and 452.29 USD separately. This data eventually confirms that the proposed SOPS approach is guaranteed to yield higher energy savings by a margin of 36 USD. It is important to mention here that the analysis is made only for 5 days and if the same is extended for a year, a monumental income generation is obvious. Additionally, the excess CAPEX cost consumed by the SOPS arrangement can be covered within 15 days, having 8 effective sun hours every day. However, the real-time soiling conditions are subject to change in outdoor environment conditions. Nonetheless, the payback returns for the excess CAPEX cost can easily be recovered in minimal time, and more importantly, the income generation is substantial.

In addition to the cost benefits, the SOPS arrangement is guaranteed to enable flexible operation between CPG and MPP mode even when soiling conditions are inevitable for PV power generation. For a better understanding of improved units and revenue generation, a bar chart to represent the quantitative comparison between the conventional and SOPS approach is presented in Fig. 11. Even though the SOPS approach has the drawback of complex wiring, the income generated from the SOPS approach is always found high. Adding to the earlier, the rewiring process is a one-time procedure, which will always ensure the reproduction of GMPP closer to V_{OC}. Moreover, the SOPS approach guarantees inverter-friendly MPP operation, which is a notable benefit in real-time PV deployment.

V. Experimental Tracking Results

The previous section demonstrates the power enhancement capabilities of the SOPS approach. However, it is mandatory to also validate the inverter-friendly tracking capability of the proposed method. Hence, a laboratory prototype comprising of ETS Terra SAS PV simulator and DC-DC Boost converter has been developed, and the proposed adaptive P&O approach is programmed to emulate real-time MPP tracking. A picture of the experimental setup built in the energy systems laboratory at POSTECH is shown in Fig.12. The current and voltage sensors designed and utilized are LA25P and LV55P respectively, whose analog values are then fed to the Arduino UNO controller to generate the control signals. For switch isolation, the Infineon EVAL-1ED44176N01F driver circuit has been employed. Other design parameters for the boost converter include switching frequency (10 kHz), (ii) inductance (1mH), (iii) capacitance (650 V, 100 μF), and (iv) load resistance (100Ω, 15A).

To align with the earlier findings and theoretical conclusions, experimental testing is also performed by considering the same PV system to derive the results. However, the current values are downsized by 50% to meet the hardware design values. Furthermore, shade patterns discussed in section IV have been used to test the proposed tracking scheme, along with some dynamic transition studies between two various shade patterns. For in-depth analysis and understanding of the power oscillations as well as the tracking speed, the results obtained are also compared with conventional P&O and adaptive P&O methods. Various parameters tuned for P&O and the developed adaptive P&O methods are presented in Table VII. For brevity, TCT interconnected shade patterns are programmed for conventional P&O methods to exemplify the importance of GMPP and RPP locations, whereas the output characteristics of the rewired array design are emulated in the PV simulator is tested with the same conventional P&O and adaptive P&O methods to contribute for a fair comparison. Comprehensive discussions pertinent to switching transients, voltage, power, and current convergence for each pattern are also presented in the forthcoming subsections.

A. Soiling Patterns 1 and 2

For soiled pattern 1, the programmed data patterns in the

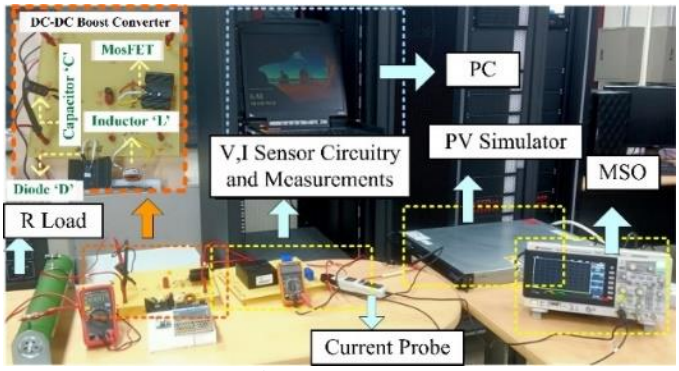

Fig.12. Laboratory prototype for experimental testing.

TABLE VII
PARAMETERS OF P&O & TWO-PHASE P&O METHOD

P&O	Two phase P&O
D=0.8	*D=0.1*
ΔD=2%	*ΔD=2% and 10%*

This article has been accepted for publication in IEEE Transactions on Power Electronics. This is the author's version which has not been fully edited and content may change prior to final publication. Citation information: DOI 10.1109/TPEL.2023.3321601

PV simulator for the TCT and rewired PV interconnection are presented in Fig.13(a) and Fig.13(b) respectively. During the trial run, the conventional P&O method is initially applied to the TCT/SP configuration, and the results obtained are presented in Fig.13(c). It can be observed that the P&O method is initialized in the constant voltage region and tracks

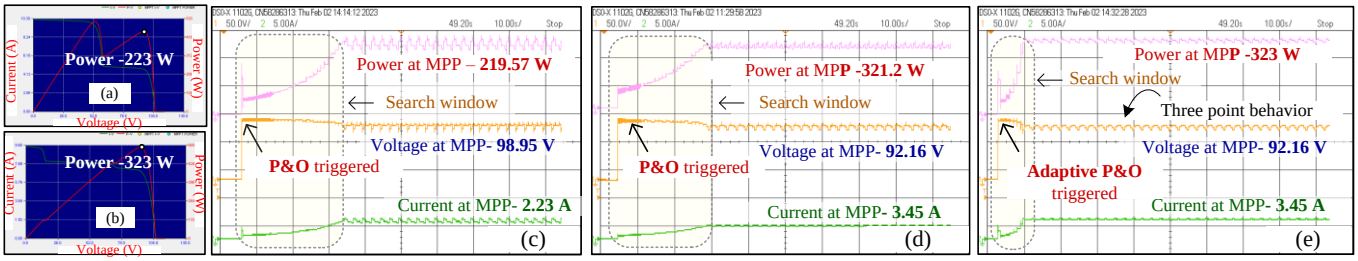

Fig.13. Programmed P-V characteristics of PV simulator (a) TCT arrangement (b) SOPS arrangement, experimental results for (c) P&O method in TCT arrangement, (d) P&O method in SOPS arrangement and (e) adaptive P&O in SOPS arrangement – soiling case 1.

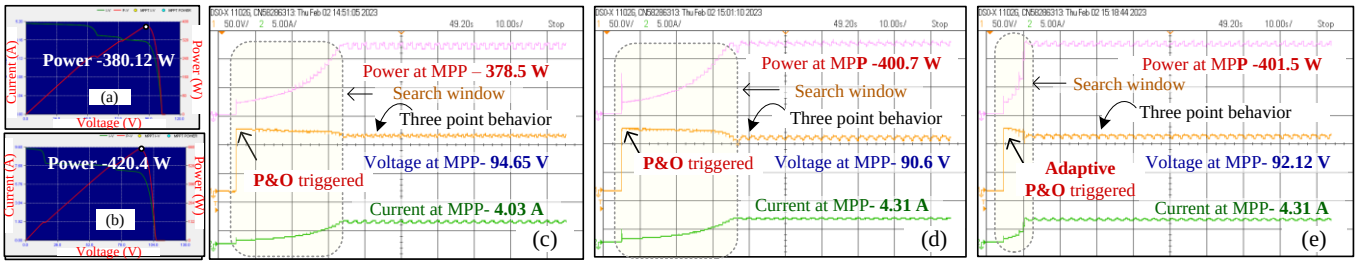

Fig.14. Programmed P-V characteristics of PV simulator (a) TCT arrangement (b) SOPS arrangement, experimental results for (c) P&O method in TCT arrangement, (d) P&O method in SOPS arrangement and (e) adaptive P&O in SOPS arrangement – soiling case 2.

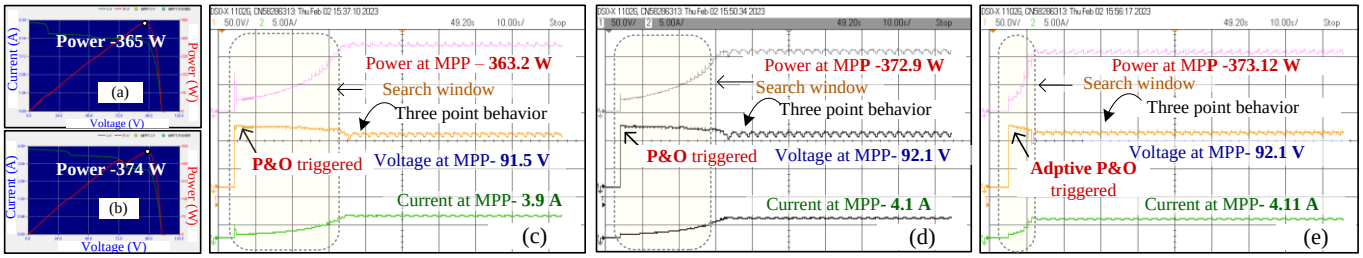

Fig.15. Programmed P-V characteristics of PV simulator (a) TCT arrangement (b) SOPS arrangement, experimental results for (c) P&O method in TCT arrangement, (d) P&O method in SOPS arrangement and (e) adaptive P&O in SOPS arrangement – soiling case 3.

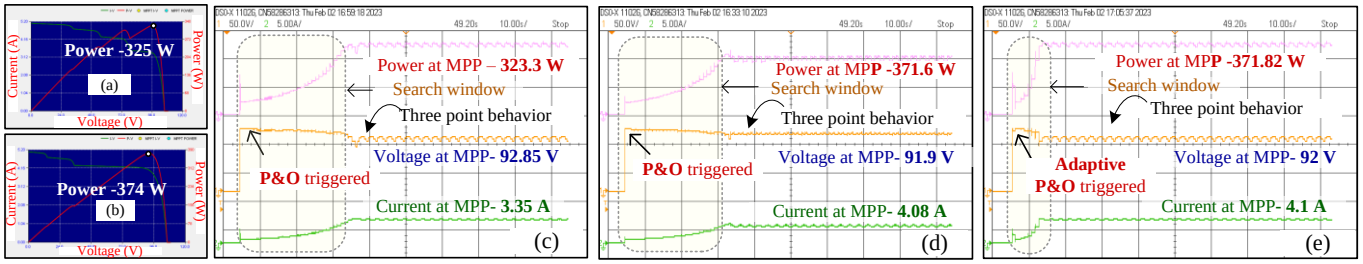

Fig.16. Programmed P-V characteristics of PV simulator (a) TCT arrangement (b) SOPS arrangement, experimental results for (a) P&O method in TCT arrangement, (d) P&O method in SOPS arrangement and (e) adaptive P&O in SOPS arrangement – soiling case 4.

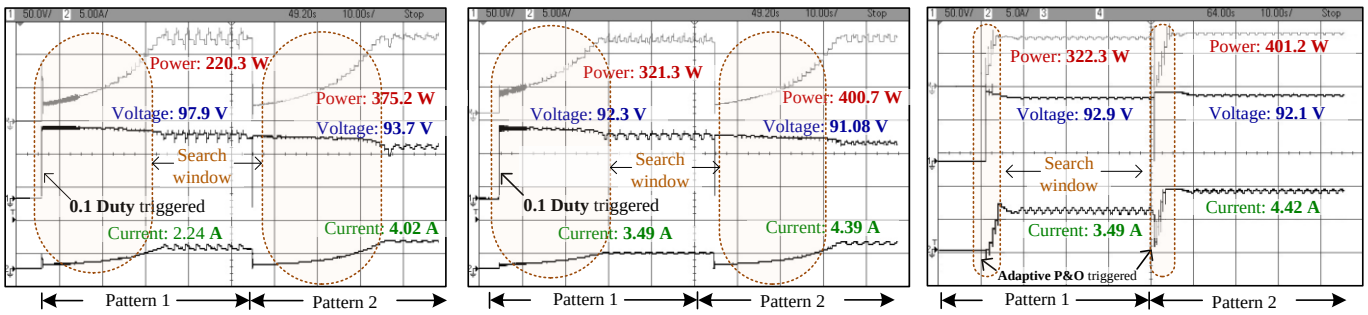

Fig.17. Experimental results for irradiation change from case 1- case 2 (a) P&O method in TCT arrangement, (d) P&O method in SOPS arrangement, and (e) adaptive P&O in SOPS arrangement.

the first immediate peak originating from the right side, which represents the LMPP (V=98.95 V, P=219.57 W). It is worth noting that if a different assumption was made regarding the previous position of the P&O algorithm, assuming it to be in the constant current region, it would have settled to the GMPP. A similar hardware implementation is shown in Fig.13(d) for the SOPS configuration. With the same duty cycle value, a significant power enhancement is observed as the SOPS approach produces 321.2 W (92.16 V, 3.46 A). It should be noted that in both cases, the tracking time (indicated as search windows) required to reach the GMPP is quite high. However, the adaptive P&O method implemented for the SOPS configuration (Fig.13(e)) showcases much faster convergence.

The I-V and P-V characteristics of the TCT and SOPS array design programmed for soiling case 2 in the PV simulator are shown in Fig.14(a) and Fig.14(b) respectively, while the tracking responses of the conventional P&O algorithm for the corresponding patterns are presented in Fig.14(c) and Fig.14(d) respectively. As can be seen, unlike case 1, the P&O algorithm has attained the GMPP for shade case 2 in the soiled TCT (380.12 W) as well as for the SOPS soiling mitigation approach (400.7 W). It is noteworthy that a comprehensive power enhancement of nearly 50 W is achieved by the SOPS implementation, and the GMPP has been relocated to the RPP itself. Furthermore, like soiling pattern 1, the adaptive P&O method exhibits superior convergence performance by reaching the GMPP within 5 samples when implemented with the SOPS configuration (Fig.14(e)). Overall, the proposed tracking scheme improves the convergence characteristics, the SOPS approach enhances the power performance, eliminates the need for entire I-V curve scanning, and reduces voltage oscillations.

B. Soiling Patterns 3 and 4

In the case of soiling pattern 3, a similar situation to case 2 is observed, where the GMPP is already located at the RPP for both the TCT and SOPS interconnection methods. However, the TCT/SP interconnection induces multiple local power peaks in the output characteristics. The programmed PV simulator characteristics for TCT and SOPS approaches are presented in Fig.15(a) and Fig.15(b) respectively. Fig.15(c) and Fig.15(d) exemplify the tracking response of the conventional P&O algorithm in the TCT interconnection (attaining P=363.2 W at 91.5 V) and SOPS interconnection (attaining P=372.9 W at 92.1 V) respectively.

While the SOPS approach demonstrates better power performance by dispersing the shade caused by soiling, the application of the proposed adaptive tracking method also improves the tracking performance. As observed in Fig.15(e), only six perturbations are required to track the GMPP located at (373.12 W, 92.1 V) when the adaptive P&O method is implemented. This showcases a power capture of 371.82 W at the RPP voltage, which is nearly equal to 92V, with minimal oscillations, convergence time, and tracking complexity.

In contrast to pattern 3, case 4 is more complex as it involves four irradiance changes, as shown in Fig. 9, resulting in four major peaks in the I-V characteristics, as depicted in Fig.16(a). However, by benefiting from the SOPS approach, the power attainment has been significantly increased, with a 52 W increment, when the array is rewired, as shown in Fig.16(b). The tracking results of the P&O method applied to the TCT and SOPS arrangements are presented in Fig.16(c) and Fig.16(d) respectively, confirming the aforementioned findings. It is important to note that for both cases, the GMPP is located at the RPP itself. On the other hand, the tracking performance is improved once the proposed two-phase adaptive P&O methods are implemented, as shown in Fig.16(e).

Dynamic Changes in Soiling Patterns:

This experiment aims to evaluate the response of the proposed tracking scheme in dynamic irradiance variations. Both the conventional P&O method and the adaptive P&O method were tested for rapid transitions from soiling case 1 to soiling case 2. The tracking responses of the P&O method applied to the dynamic variations in the TCT and SOPS interconnections are presented in Fig.17(a) and Fig.17(b) respectively.

It is observed that the P&O method achieves convergence with power differences of 100 W and 25 W in cases 1 and 2 respectively. However, by implementing the adaptive P&O method, the GMPPs of case 1 (323.3 W, 92.9 V) and case 2 (401.2 W, 92.1 V) are tracked faster (see Fig.17(c)) with fewer voltage oscillations. This improved tracking effectiveness can be clearly understood by comparing the search windows for the three cases, which are almost 25% of the conventional tracking duration for the proposed approach.

VI. Conclusions

In this work, a new PV array design that always guarantees GMPP operation and inverter-friendly power tracking in non-homogenously soiled/shaded PV arrays has been proposed. Furthermore, to address the limitations associated with conventional P&O, an adaptive P&O tracking methodology (flexible) was proposed. The investigations performed have highlighted the feasibility of the SOPS rewiring approach to transform RPP to GMPP during complex shade/soiled conditions. This subsequently has proven to be a viable approach to track GMPP more efficiently by inverters. Also, experimental evaluations suggested that the proposed adaptive P&O method improves the convergence characteristics as well. Though out of scope, the findings in this article also have key applications to flexible power tracking in grid-connected systems, that could allow constant power generation operation at GMPP even during partial shade conditions.

References

[1] D. S. Pillai, J. P. Ram, V. Shabunko, and Y. J. Kim, “A new shade dispersion technique compatible for symmetrical and unsymmetrical photovoltaic (PV) arrays,” *Energy*, vol. 225, Jun. 2021.

[2] Y. Yang, H. Wang, F. Blaabjerg, and T. Kerekes, “A hybrid power control concept for PV inverters with reduced thermal loading,” *IEEE Trans. Power Electron.*, vol. 29, no. 12, pp. 6271–6275, 2014.

[3] K. Ilse *et al.*, “Techno-Economic Assessment of Soiling Losses and Mitigation Strategies for Solar Power Generation,” *Joule*, vol. 3, no. 10, pp. 2303–2321, Oct. 2019.

[4] M. Killi and S. Samanta, “Modified Perturb and Observe MPPT Algorithm for Drift Avoidance in Photovoltaic Systems; Modified Perturb and Observe MPPT Algorithm for Drift Avoidance in Photovoltaic Systems,” *IEEE Trans. Ind. Electron.*, vol. 62, p. 5549, 2015.

[5] K. S. Tey and S. Mekhilef, “Modified Incremental Conductance Algorithm for Photovoltaic System Under Partial Shading Conditions and Load Variation,” *IEEE Trans. Ind. Electron.*, vol. 61, no. 10, 2014.

[6] D. S. Pillai and N. Rajasekar, "An MPPT-based sensorless line-line and line-ground fault detection technique for pv systems," *IEEE Trans. Power Electron.*, vol. 34, no. 9, pp. 8646–8659, Sep. 2019.

[7] K. Ishaque, Z. Salam, M. Amjad, and S. Mekhilef, "An Improved Particle Swarm Optimization (PSO) based MPPT for PV With Reduced Steady-State Oscillation," *IEEE Trans. Power Electron.*, vol. 27, no. 8, p. 3627, 2012.

[8] J. Prasanth Ram and N. Rajasekar, "A Novel Flower Pollination Based Global Maximum Power Point Method for Solar Maximum Power Point Tracking," *IEEE Trans. Power Electron.*, vol. 32, no. 11, 2017.

[9] R. Motamarri and N. Bhookya, "JAYA Algorithm Based on Lévy Flight for Global MPPT Under Partial Shading in Photovoltaic System," *IEEE J. Emerg. Sel. Top. Power Electron.*, vol. 9, no. 4, p. 4979, 2021.

[10] M. Seyedmahmoudian *et al.*, "Simulation and Hardware Implementation of New Maximum Power Point Tracking Technique for Partially Shaded PV System Using Hybrid DEPSO Method," *IEEE Trans. Sustain. Energy*, vol. 6, no. 3, 2015.

[11] C. Manickam *et al.*,"Fireworks Enriched P&O Algorithm for GMPPT and Detection of Partial Shading in PV Systems," *IEEE Trans. Power Electron.*, vol. 32, no. 6, 2017.

[12] K. Sundareswaran, S. Peddapati, and S. Palani, "MPPT of PV Systems Under Partial Shaded Conditions Through a Colony of Flashing Fireflies," *IEEE Trans. Energy Convers.*, vol. 29, no. 2, p. 463, 2014.

[13] K. Sundareswaran *et al.*, "Development of an Improved P&O Algorithm Assisted Through a Colony of Foraging Ants for MPPT in PV System," *IEEE Trans. Ind. Informatics*, vol. 12, no. 1, p. 187, 2016,.

[14] A. Ostadrahimi, and Y. Mahmoud, "Novel Spline-MPPT Technique for Photovoltaic Systems Under Uniform Irradiance and Partial Shading Conditions; Novel Spline-MPPT Technique for Photovoltaic Systems Under Uniform Irradiance and Partial Shading Conditions," *IEEE Trans. Sustain. Energy*, vol. 12, no. 1, 2021.

[15] J. P. Ram, T. S. Babu, and N. Rajasekar, "A comprehensive review on solar PV maximum power point tracking techniques," *Renew. Sustain. Energy Rev.*, vol. 67, pp. 826–847, 2017,.

[16] C. Manickam *et.al.*, "A Hybrid Algorithm for Tracking of GMPP Based on P&O and PSO With Reduced Power Oscillation in String Inverters" *IEEE Trans. Ind. Electron.*, vol. 63, no. 10, p. 6097, 2016,.

[17] R. Kadri, J.-P. Gaubert, and G. Champenois, "An Improved Maximum Power Point Tracking for Photovoltaic Grid-Connected Inverter Based on Voltage-Oriented Control," *IEEE Trans. Ind. Electron.*, vol. 58, no. 1, 2011.

[18] I. Pervez *et al.*, "Most Valuable Player Algorithm based Maximum Power Point Tracking for a Partially Shaded PV Generation System," *IEEE Trans. Sustain. Energy*, vol. 12, no. 4, 2021.

[19] A. Sangwongwanich, Y. Yang, F. Blaabjerg, and H. Wang, "Benchmarking of Constant Power Generation Strategies for Single-Phase Grid-Connected Photovoltaic Systems," *IEEE Trans. Ind. Appl.*, vol. 54, no. 1, pp. 447–457, Jan. 2018.

[20] A. Sangwongwanich, Y. Yang, and F. Blaabjerg, "High-performance constant power generation in grid-connected PV systems," *IEEE Trans. Power Electron.*, vol. 31, no. 3, pp. 1822–1825, Mar. 2016.

[21] A. Sangwongwanich, Y. Yang, and F. Blaabjerg, "A Sensorless Power Reserve Control Strategy for Two-Stage Grid-Connected PV Systems," *IEEE Trans. Power Electron.*, vol. 32, no. 11, pp. 8559–8569, Nov. 2017.

[22] S. B. Kjaer, J. K. Pedersen, and F. Blaabjerg, "A review of single-phase grid-connected inverters for photovoltaic modules," *IEEE Trans. Ind. Appl.*, vol. 41, no. 5, pp. 1292–1306, 2005.

[23] K. Alluhaybi, I. Batarseh, and H. Hu, "Comprehensive Review and Comparison of Single-Phase Grid-Tied Photovoltaic Microinverters," *IEEE J. Emerg. Sel. Top. Power Electron.*, vol. 8, no. 2, pp. 1310–1329, 2020.

[24] G. Sai Krishna and T. Moger, "Optimal SuDoKu Reconfiguration Technique for Total-Cross-Tied PV Array to Increase Power Output under Non-Uniform Irradiance," *IEEE Trans. Energy Convers.*, 2019.

[25] T. S. Babu *et al.*, "Particle swarm optimization based solar PV array reconfiguration of the maximum power extraction under partial shading conditions," *IEEE Trans. Sustain. Energy*, vol. 9, no. 1, pp. 74–85, 2018.

[26] M. S. S. Nihanth *et al.*,"Enhanced power production in PV arrays using a new skyscraper puzzle based one-time reconfiguration procedure under partial shade conditions (PSCs)," *Sol. Energy*, vol. 194, pp. 209–224, Dec. 2019.

[27] J. Ahmed and Z. Salam, "An Enhanced Adaptive P&O MPPT for Fast and Efficient Tracking Under Varying Environmental Conditions," *IEEE Trans. Sustain. Energy*, vol. 9, no. 3, pp. 1487–1496, Jul. 2018.

[28] S. Malathy and R. Ramaprabha, "Reconfiguration strategies to extract maximum power from photovoltaic array under partially shaded conditions," *Renewable and Sustainable Energy Reviews*. 2018.

[29] Kazem, H.A., Chaichan, M.T., Al-Waeli, A.H. and Sopian, K. " A review of dust accumulation and cleaning methods for solar photovoltaic systems". *Journal of Cleaner Production*, 2020,Vol.*276*, pp.123187.

[30] S36 datasheet, "Product Information Sheet Shell SM50-H Module Shell SM50-H Typical I / V Characteristics," pp. 75–76, 2003.

Dhanup S. Pillai (M'18) received the B.Tech degree in Electrical and Electronics Engineering from Mahatma Gandhi University, Kerala, India, in 2010, the ME degree in Power Electronics and Drives from Anna University, Tamil Nadu, India, in 2015 and the Ph.D. degree in Electrical Engineering from Vellore Institute of Technology (VIT), Vellore, India, in 2019 respectively. He was a Postdoctoral Research Fellow with the School of Electrical and Electronic Engineering, Nanyang Technological University, Singapore during 2019-2020 and Research Fellow with the Solar Energy Research Institute of Singapore (SERIS) - National University of Singapore during 2020-2022. He is currently working as a scientist with the Energy Center at the Qatar Environment and Energy Research Institute (QEERI), Doha - Qatar. His research interests include PV module and system reliability, fault detection, protection, soiling/shade detection and mitigation, power electronics for PV systems, and building integrated photovoltaic systems (BIPV).

J. Prasanth Ram (M'23) received his B.E. degree in Electrical and Electronics Engineering in 2012 from Bannari Amman Institute of Technology, Sathyamangalam, India., the M.E. degree in Power Electronics and Drives in 2014 from Kumaraguru College of Technology, Coimbatore, India and the Ph.D degree from Vellore Institute of Technology (VIT) –Vellore, India respectively. He is currently working as post-doctoral researcher at Pohang University of Science and Technology (POSTECH), South Korea. His areas of interest include PV fault diagnosis, PV maximum power point tracking, Optimization techniques, smart grid, energy management systems, and of power electronics application in PV energy conversion. He is the recipient of Brain Pool research fellowship for the year 2020-2024, a fellowship provided by National Research Foundation of Korea (NRF) funded by the Ministry of Science and ICT – South Korea (2020H1D3A1A04079991).

Juan Lopez-Garcia is Principal Investigator and Research Program Director for the energy conversion program in the Energy Center at the Qatar Environment and Energy Research Institute (QEERI), Qatar. He received the MSc in Science (physics) from the Autonomous University of Madrid, Spain, and the Ph.D. in Applied Physics from the same university and the Research Centre for Energy, Environment and Technology (CIEMAT), Madrid (Spain) in 2010. He worked as Research Scientist at the Research Centre for Energy, Environment and Technology (CIEMAT), Madrid and the Catalan Institute of Energy Research (IREC), Barcelona (Spain). He was also Scientific Project Officer of the European Commission in the Joint Research Centre (JRC) at Ispra (Italy) working on the European Solar Test Installation (ESTI). Dr. Lopez-Garcia is author or co-author of more than 96 scientific contributions, member of international scientific committees and he has been awarded with several best contributions award in renowned conferences.

Young-Jin Kim (Senior Member, IEEE) received the B.S. and M.S. degrees in electrical engineering from Seoul National University, Seoul, South Korea, in 2007 and 2010, respectively, and the Ph.D. degree in electrical engineering from the Massachusetts Institute of Technology, Cambridge, MA, USA, in 2015. From 2007 to 2011, he was with Korea Electric Power Corporation as a Power Transmission and Distribution System Engineer. He was also a Visiting Scholar with the Catalonia Institute for Energy Research in 2014, and a Postdoctoral Researcher with the Center for Energy, Environmental, and Economic Systems Analysis, Energy Systems Division, Argonne National Laboratory from 2015 to 2016. He joined the Faculty with the Pohang University of Science and Technology, where he is currently an Associate Professor with the Department of Electrical Engineering. His research interests include distributed generators, renewable energy resources, and smart buildings.

João P. S. Catalão (Fellow, IEEE) received the M.Sc. degree from the Instituto Superior Técnico (IST), Lisbon, Portugal, in 2003, and the Ph.D. degree and Habilitation for Full Professor ("Agregação") from the University of Beira Interior (UBI), Covilha, Portugal, in 2007 and 2013, respectively. Currently, he is a Professor at the Faculty of Engineering of the University of Porto (FEUP), Porto, Portugal. He was the Primary Coordinator of the EU-funded FP7 project SiNGULAR, a 5.2-million-euro project involving 11 industry partners. He has authored or coauthored more than 500 journal publications and 400 conference proceedings papers, with an *h*-index of 92 and more than 32,000 citations (according to Google Scholar), having supervised more than 120 post-docs, Ph.D. and M.Sc. students, and other students with project grants. He was the General Chair and General Co-Chair of SEST 2019 and SEST 2020, respectively, after being the inaugural Technical Chair and co-founder of SEST 2018. He is a Senior Editor of the IEEE TRANSACTIONS ON NEURAL NETWORKS AND LEARNING SYSTEMS. Furthermore, he is an Associate Editor of nine other IEEE TRANSACTIONS/JOURNALS. He was an IEEE Computational Intelligence Society (CIS) Fellows Committee Member in 2022 and 2023. He was recognized as one of the Outstanding Associate Editors 2020 of the IEEE TRANSACTIONS ON SMART GRID, and one of the Outstanding Associate Editors 2021 of the IEEE TRANSACTIONS ON POWER SYSTEMS. He has multiple Highly Cited Papers in Web of Science. He has won 5 *Best Paper Awards* at IEEE Conferences. Furthermore, he was the recipient of the 2017-2022 (for the sixth consecutive year) FEUP Scientific Recognition Diplomas. His research interests include power system operations and planning, power system economics and electricity markets, distributed renewable generation, demand response, smart grid, and multi-energy carriers.